The Journal of Experimental Biology 199, 2139–2151 (1996)
Printed in Great Britain © The Company of Biologists Limited 1996
JEB0356

FUNCTIONS OF FISH SKIN: FLEXURAL STIFFNESS AND STEADY SWIMMING OF LONGNOSE GAR *LEPISOSTEUS OSSEUS*

JOHN H. LONG, JR[1,*], MELINA E. HALE[2], MATT J. MCHENRY[1] AND MARK W. WESTNEAT[3]

[1]*Department of Biology, Vassar College, Poughkeepsie, NY 12601, USA*, [2]*Department of Organismal Biology and Anatomy, University of Chicago, Chicago, IL 60637, USA* and [3]*Center for Evolutionary and Environmental Biology, Field Museum of Natural History, Chicago, IL 60605, USA*

Accepted 17 June 1996

Summary

The functions of fish skin during swimming remain enigmatic. Does skin stiffen the body and alter the propagation of the axial undulatory wave? To address this question, we measured the skin's *in situ* flexural stiffness and *in vivo* mechanical role in the longnose gar *Lepisosteus osseus*. To measure flexural stiffness, dead gar were gripped and bent in a device that measured applied bending moment (N m) and the resulting midline curvature (m^{-1}). From these values, the flexural stiffness of the body (*EI* in $N m^2$) was calculated before and after sequential alterations of skin structure. Cutting of the dermis between two caudal scale rows significantly reduced the flexural stiffness of the body and increased the neutral zone of curvature, a region of bending without detectable stiffness. Neither bending property was significantly altered by the removal of a caudal scale row. These alterations in skin structure were also made in live gar and the kinematics of steady swimming was measured before and after each treatment. Cutting of the dermis between two caudal scale rows, performed under anesthesia, changed the swimming kinematics of the fish: tailbeat frequency (Hz) and propulsive wave speed (body lengths per second, $L s^{-1}$) decreased, while the depth (in *L*) of the trailing edge of the tail increased. The decreases in tailbeat frequency and wave speed are consistent with predictions of the theory of forced, harmonic vibrations; wave speed, if equated with resonance frequency, is proportional to the square root of a structure's stiffness. While it did not significantly reduce the body's flexural stiffness, surgical removal of a caudal scale row resulted in increased tailbeat amplitude and the relative total hydrodynamic power. In an attempt to understand the specific function of the scale row, we propose a model in which a scale row resists medio-lateral force applied by a single myomere, thus functioning to enhance mechanical advantage for bending. Finally, surgical removal of a precaudal scale row did not significantly alter any of the kinematic variables. This lack of effect is associated with a lower midline curvature of the precaudal region during swimming compared with that of the caudal region. Overall, these results demonstrate a causal relationship between skin, the passive flexural stiffness it imparts to the body and the influence of body stiffness on the undulatory wave speed and cycle frequency at which gar choose to swim.

Key words: skin, scales, ganoid scales, swimming, undulation, undulatory waves, flexibility, stiffness, locomotion, longnose gar, *Lepisosteus osseus*.

Introduction

Aquatic propulsion in many fishes is driven by the progression down the body of alternating lateral flexures. These traveling waves of bending, driven by muscle, alternately stretch and compress the body's axial structures. The structure likely to undergo the largest reconfigurations, because of its distance from the bending axis of the backbone, is the skin. The skin is in a position to influence, by means of its mechanical properties, much of the body's undulatory motion. For this reason, we sought to understand the mechanical functions of the skin during swimming. In this study, we tested locomotor hypotheses using *in vivo* surgical manipulation of skin structure and *in situ* measurement of the flexural stiffness of the body.

In addition to its anatomical position, several other characteristics of fish skin make its study compelling. First, fish skin varies widely in structure, bearing large ganoid scales in gars (Lepistosteidae) and polypterids (Polypteridae), small scales in sharks (Elasmobranchii) and tunas (Scombridae), and no scales in swordfish (Xiphiidae) and some catfishes (Siluriformes) (Kerr, 1952; Pearson, 1981; Nelson, 1984). In spite of these differences, fish skin appears to possess an underlying structural ground plan – cross-helical fibers of

*e-mail: jolong@vassar.edu.

collagen embedded in the dermis (e.g. Fujii, 1968; Motta, 1977; Videler, 1974; Pearson, 1981). Second, skin has a complex two-dimensional stiffness. Circumferential strain stiffens it axially, giving it the capability to transmit axial forces in lemon sharks *Negaprion brevirostris* (Wainwright *et al.* 1978) and eels *Anguilla rostrata* (Hebrank, 1980); however, this capability is lacking in spot *Leiostomus xanthurus* and skipjack tuna *Katsuwonus pelamis* (Hebrank and Hebrank, 1986). Third, skin is attached directly to the underlying muscles, putting it in series between muscle and propulsive elements (Pearson, 1981; Westneat *et al.*1993; Hale, 1996).

The role of skin during swimming has been addressed comparatively. The armored skin of longnose gar *Lepisosteus osseus*, with its heavy ganoid scales, is associated with reduced swimming performance during fast starts (Webb *et al.* 1992). When compared with the lightly scaled tiger musky, *Esox lucius* × *Esox masquinongy*, gar cover less distance during the early stages of the fast start (Webb *et al.* 1992). This discrepancy was thought to be caused by the presence of less myotomal muscle mass in gar (38 *versus* 53 % of total body mass for gar and musky, respectively), leaving gar with only 72 % of the force-generating capabilities of musky. Thus, gar appear to trade muscle mass for skin mass, which leaves them with higher inertia but greater passive predator defense during unsteady swimming. In contrast, Webb *et al.* (1992) detected no differences in performance during steady swimming that could be attributed to differences in muscle mass. Similar power coefficients and body curvature in both species did not support the hypothesis that armored skin would increase the cost of steady swimming and decrease the flexibility of the body. However, gar swam at much lower critical swimming speeds than did musky (1.9 *versus* $3.4\,L\,s^{-1}$), a difference than cannot be accounted for by the muscle mass difference alone.

Given the potential importance of skin as a locomotor organ, we asked (1) how the skin affects the flexural stiffness of the body and (2) how the skin functions during steady swimming. In terms of the stiffness of the body when the muscles are not operating, termed passive stiffness, we tested two hypotheses. First, we hypothesized that skin should add little to the passive stiffness of the body because of its cross-helical fiber arrangement, which renders a low longitudinal (axial) stiffness (Videler, 1993). Because this hypothesis is based on *in vitro* measurements, however, an alternative is possible – skin may stiffen the body in axial compression, tension and torsion because its bony scales and attachments to underlying myomeres do not permit it to act as a simple, cross-helical cylinder (Pearson, 1981). In the first case, we predict that any circumferential cut in the skin would not affect the body's passive flexural stiffness (*EI*, in $N\,m^2$); in the second case, we predict that such an effect will occur.

In terms of function during swimming, the flexural stiffness imparted to the body by the skin may play a role in determining the cycle frequency and propulsive wave speed at which the fish chooses to operate (Long and Nipper, 1996). This wave speed hypothesis follows from work on swimming fish models, which have an undulatory wave speed determined by the flexural stiffness of their bodies (McHenry *et al.* 1995). We predict that any circumferential cut in the skin, provided that such cuts reduce body stiffness, should alter wave speed in proportion to the change in flexural stiffness. Since wave speed is the product of tailbeat frequency and propulsive wavelength, we would expect to see either kinematic variable decrease with decreases in body stiffness. To maintain thrust power at a given swimming speed with lower body stiffness, either tailbeat amplitude or tail depth (trailing-edge span in the dorso-ventral plane) should increase (see Webb *et al.* 1984; Wu, 1977).

We tested these predictions in longnose gar because their armored skin, which bears robust ganoid scales (Kerr, 1952), is thought to decrease body flexibility and swimming performance (see Webb *et al.* 1992). In intact, freshly killed gar, we measured the flexural stiffness of the body before and after cutting the dermis and removing scale rows. This method has the advantage of subjecting skin to more realistic strains compared with *in vitro* bi-axial tests in which excised skin is stretched independently of underlying muscle and connective tissue. We also measured the swimming performance of live gar before and after surgical treatments in which the fibrous dermis was cut and scale rows were removed. This procedure has the advantage of comparing different skin configuration conditions within a single species.

Materials and methods

Animals

Longnose gar *Lepisosteus osseus* Linnaeus were collected from Sweetwater Creek, Martin County, North Carolina, USA, using gill nets. Once set, nets were monitored continually to minimize the amount of time any individual spent entangled. Within 8 h of capture, fish were transported to the Duke University Marine Laboratory, where they were placed in outdoor holding tanks with water temperatures between 22 and 30 °C. Fish were kept for no longer than 2 weeks, during which time they were not fed. The three individuals used for the swimming experiments were 46, 50 and 76 cm total body length (*L*, tip of rostrum to tip of tail). The three individuals used for the bending experiments were 64, 64 and 71 cm *TL*.

Stiffness tests

To measure the mechanical effect of each of the surgical treatments on the passive bending stiffness of the gar's body, the following tests were conducted. Three freshly killed individuals were mounted in and bent on a testing machine modified from Long (1992). The region of the body at the site of the first ('dermis cut' treatment) and second ('caudal scale row' treatment) surgical treatments was chosen for examination (Figs 1, 2); the site of the third ('precaudal scale row') surgical treatment could not be tested since this region was altered by the gripping procedure. The gar's body was gripped anterior and posterior to the test site by epoxy-

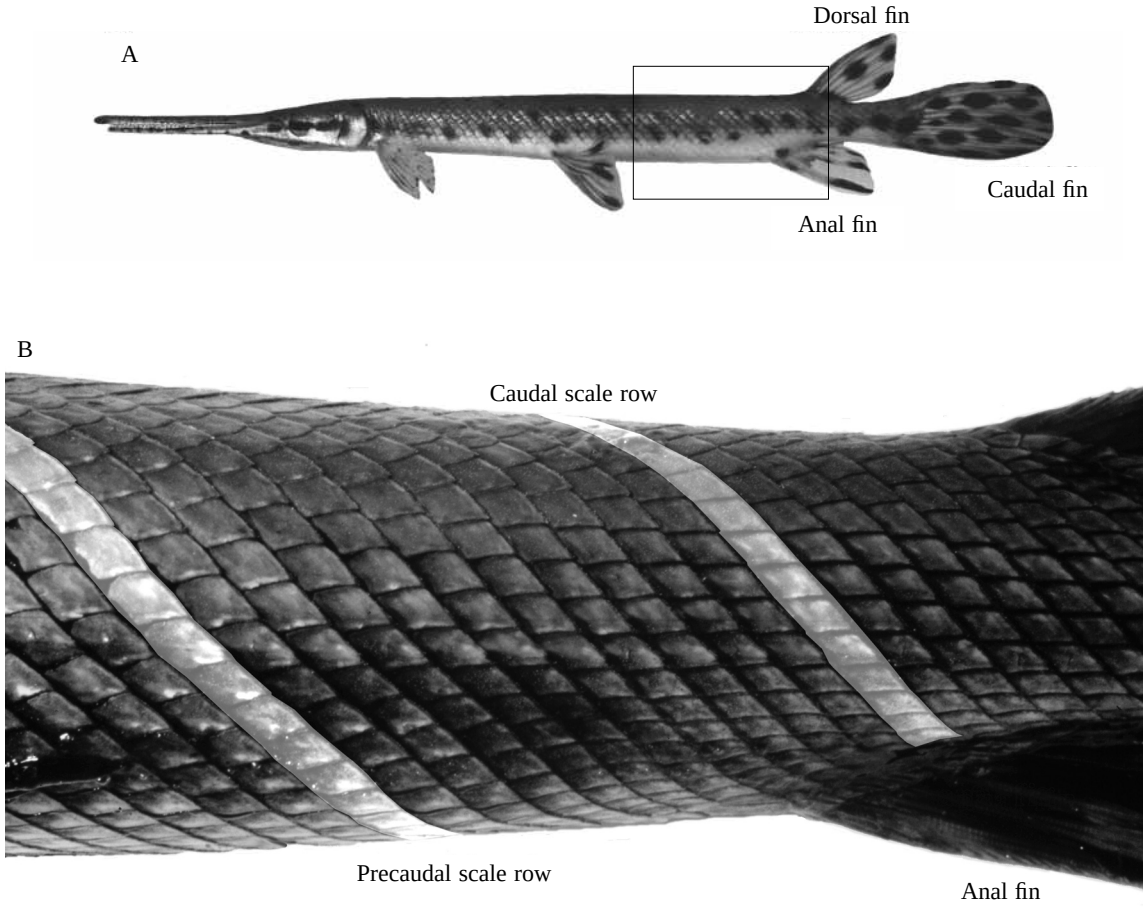

Fig. 1. Sites of skin surgery (left lateral view). (A) Longnose gar *Lepisosteus osseus* (46 cm individual) with region of surgical manipulation of skin highlighted by superimposed rectangle. (B) Detail of surgical sites in a preserved specimen. The caudal scale row is the location of the first surgical treatment, in which the dermis was cut bilaterally between the eighth and ninth scale rows anterior to the dorsal fin ('dermis cut' treatment). At this same site, subsequent surgery removed the entire eighth scale row on both sides (highlighted, 'caudal scale row' treatment). The final surgical treatment took place at the precaudal scale row, where the dermis was cut and the scale row (highlighted) was removed in one treatment ('precaudal scale row' treatment).

embedded sand cradled in wooden holders that were, in turn, rigidly affixed to the bending machine. The epoxy-embedded sand provided a gripping surface of even pressure distribution and contoured shape.

Each gar was bent quasi-statically at frequencies below 1 Hz. The bending moment (N m) and angular displacement (rad) of the rotating portion of the machine were sampled digitally at 10 Hz using LabVIEW software (National Instruments) and an analog-to-digital converter (National Instruments, model NB-MIO-16L) mounted in a microcomputer (Apple Corporation, model Centris 650). After measuring the unaltered gar, flexural stiffness was measured after the dermis had been cut and finally after the caudal scale row had been removed. Statistical differences between treatments were tested using an analysis of variance (ANOVA) design similar to that described below for swimming kinematics, with individual and skin treatment as the independent variables. Two planned contrasts, unaltered *versus* dermis cut and dermis cut *versus* caudal scale row removed, tested differences between means.

From the graph of bending moment and angular displacement, flexural stiffness (N m^2) was calculated using beam theory (Fig. 3). A structure's flexural stiffness, the product of the Young's modulus, E, and the second moment of area, I, is related to an externally applied bending moment, M, in the following manner (Wainwright *et al.* 1976):

$$M = EI/R, \quad (1)$$

where R is the radius of curvature (in m) of the bending section. Since the radius of curvature is the inverse of the curvature, κ (in m^{-1}), substitution and rearrangement show that flexural stiffness, EI, is the proportionality constant, or slope, between the bending moment and curvature:

$$M = (EI)\kappa. \quad (2)$$

Thus, by finding the instantaneous slope of the line relating bending moment to curvature, we determined the flexural stiffness (Fig. 3). Curvature was calculated from the angular displacement in a manner identical to that described below for swimming kinematics (the inverse of R in equation 3), with the

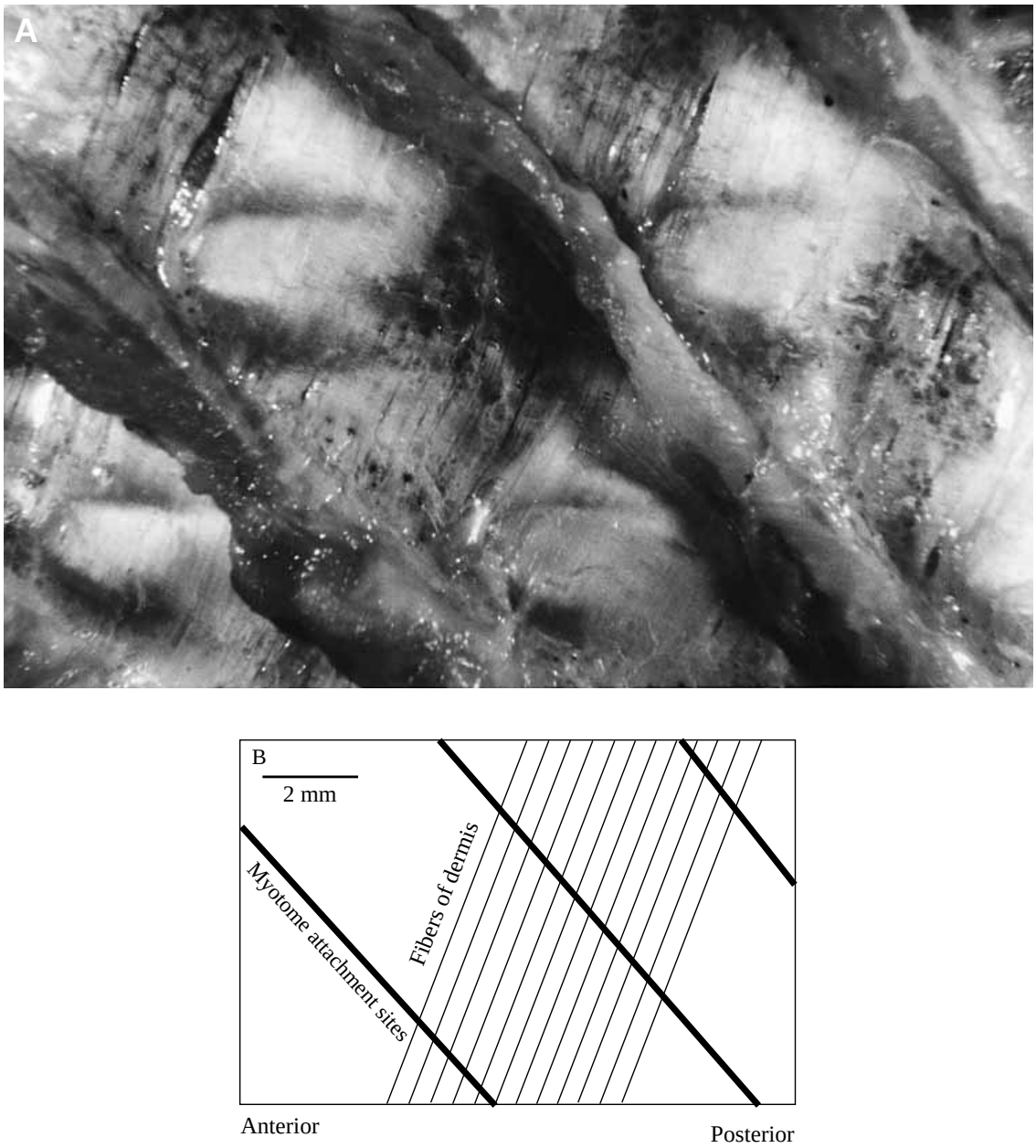

Fig. 2. Dermal fibers of skin (medial view). The dermis is organized as a sheet of parallel fibers oriented helically in the direction opposite to that of the discrete hypaxial attachments of the myotomes. The lateral surface of the dermal fibers attaches to the bony scale rows, which are oriented in the direction of the oppositely handed helix. (A) Photograph of medial hypaxial surface of skin. (B) Diagrammatic representation of A showing orientation of dermal fibers.

length of the section between the grips taken as the length, D, and θ as the angular displacement of the section. The flexural stiffness was compared for each individual and treatment at a curvature of $10\,m^{-1}$ beyond the neutral zone of curvature, which is described below. This curvature (neutral zone plus $10\,m^{-1}$) was chosen for the measurement of flexural stiffness because it approaches the extreme physiological range of curvatures measured during swimming (see Fig. 3 and Results). We thus maximize the chance of detecting physiologically meaningful differences.

In addition to flexural stiffness, the neutral zone of curvature (m^{-1}) was also measured (Fig. 3). The neutral zone of curvature is a region of little or no detectable flexural stiffness (within our resolution of $0.001\,N\,m^2$) that is symmetrical on either side of the straight (zero curvature) position of the body. The end of the neutral zone was defined as the point prior to that at which the bending moment signal was large enough to be discriminated from zero.

Experimental design

In order to test the hypothesis that the flexural stiffness imparted by the skin to the body plays a functional role during

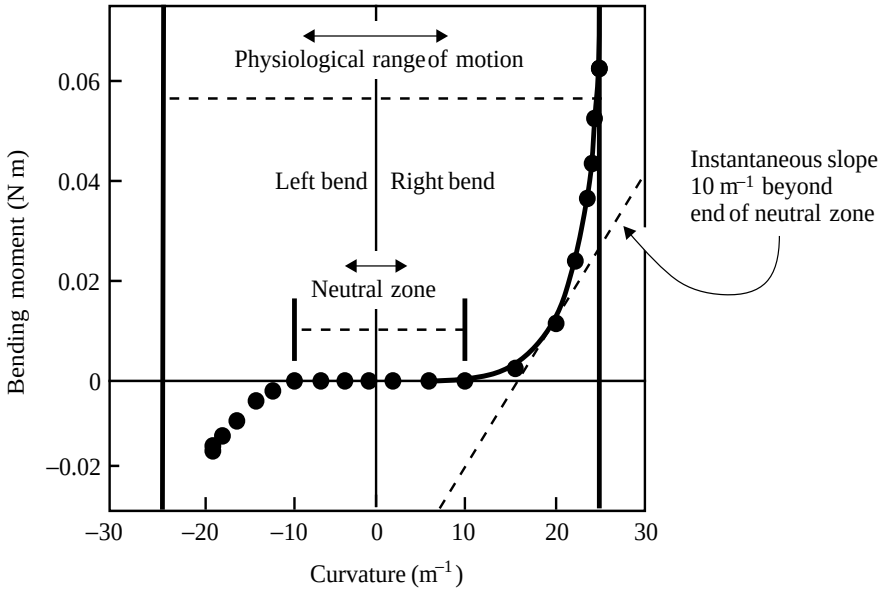

Fig. 3. Two measures of flexural stiffness. Typical loading curve from a quasi-static bending test of an intact gar body. The neutral zone of curvature is defined as the symmetrical region about zero curvature in which there is no detectable bending moment; in other words, the neutral zone is when the slope of the line, and hence the stiffness, is 0. A detectable slope is the flexural stiffness at that curvature (see equation 2). The flexural stiffness measured for comparison between skin treatments was that 10 m^{-1} beyond the end of the neutral zone. This curvature was chosen for comparison of flexural stiffness because it is at or near the maximum axial midline curvatures measured at this position on the body during swimming (see Fig. 6D). The slope of the line at that curvature is calculated from the first derivative of the polynomial regression line chosen to fit the loading curve (solid curved line).

swimming, we developed the following protocol. First, we swam individual fish at body-length-specific steady swimming speeds ranging from 0.250 to 1.000 L s^{-1} in increments of 0.125 L s^{-1}. An individual was then anesthetized using a 1:10 000 dilution of tricaine (MS-222, Argent Chemical Laboratories); following full sedation (as defined by Summerfelt and Smith, 1990), surgery commenced. In the first surgical treatment, the dermis was cut bilaterally between the caudal scale row eight rows anterior to the dorsal fin and its posterior neighbor (Figs 1, 2; 'dermis cut' treatment). This position was chosen because we expected greater axial curvature, and hence skin strain, in the caudal region relative to the precaudal region (Jayne and Lauder, 1995*b*); also, if skin transmits force to propulsive elements, this scale row should occupy a critical position, being attached posterio-ventrally to the anal fin, which contributes substantially to the production of mechanical power during swimming in gar (Webb *et al.* 1992). During surgery, care was taken to avoid damaging underlying muscle tissue. The individual was allowed to recover and was video-taped swimming once it had regained full equilibrium and motor control.

For the second surgical treatment, full sedation was again induced and the caudal scale row posterior to the cut dermis was removed bilaterally (Fig. 1; 'caudal scale row' treatment). Care was taken to avoid cutting blood vessels. The individual was allowed to recover fully and was then video-taped swimming. During the final surgical treatment, we removed a second scale row, the nineteenth anterior to the dorsal fin (Fig. 1; 'precaudal scale row' treatment). The precaudal scale row treatment combined the effects of the first two surgical treatments, since both the dermal incision and scale row removal were completed simultaneously. None of these surgical treatments took more than 20 min and they always involved two investigators, one to perform the surgery and another to monitor the condition of the fish. All three fish recovered from these treatments; after the last series of swimming events, the fish were killed with an overdose of tricaine. To control for the effects of anesthesia, we swam three different individuals that were sedated and handled as if we were performing the aforementioned surgical procedures. Prior to and following the sham surgery, we measured the swimming kinematics of these individuals; no significant differences were detected.

To test the hypothesis that the treatments described above altered the swimming kinematics of the gar, we performed a mixed-model three-way ANOVA, with individual, swimming speed ('speed') and experimental treatment of the skin ('skin') as the independent variables. All three of these variables were categorical, with individual being the random effect and speed and skin being fixed effects. The interaction of speed and skin was also tested. Individual was analogous to a randomized block effect and, when treated as a main effect, compensated for the within-individuals, repeated-measures design by removing from the error term the variance component caused by individuals (Sokal and Rohlf, 1981). The effects on response variables, which are described in the next section, were tested separately as univariate models; differences between the means of treatment categories were tested with planned *a priori* contrasts. Prior to statistical testing, the distribution of each response variable was checked for normality by examining residuals, a probability plot, skewness and kurtosis. One variable, total relative power, was transformed to achieve a normal distribution by calculating its natural logarithm. Of the 84 possible data points in this design (three individuals, seven speeds, four skin treatments), four cells were missing for reasons given in the next section. The 46 cm gar was missing one cell – precaudal scales at 0.250 L s^{-1}. The 50 cm gar was missing one cell – unaltered skin at 0.250 L s^{-1}. The 74 cm gar was missing two cells – caudal scales at 0.875 L s^{-1} and precaudal scales at 0.375 L s^{-1}. All statistical tests were conducted using SAS (SAS Institute, 1985).

Kinematics of swimming

We swam gar over a range of swimming speeds in a large flow tank (enlarged and modified from that described by Vogel, 1981) at the Duke University Marine Laboratory. The working section of the flow tank was 1 m×1 m in cross section and 3 m long. The gap-to-span ratio of the tail was always greater than 2, which ensured that individuals did not benefit energetically from wall effects (Webb, 1993). Maximum speeds in this study ($1.0\,L\,s^{-1}$) were limited by the top speed of the flow tank ($80\,cm\,s^{-1}$). This maximum speed is roughly half the critical swimming speed ($1.9\,L\,s^{-1}$) measured in longnose gar (Webb *et al.* 1992).

Using a mirror mounted at 45° above the tank, swimming fish were video-taped (Panasonic model AG-450) at 60 images s^{-1} at a shutter speed of 0.001 s from above and from a lateral perspective perpendicular to the longitudinal axis of the fish. To quantify swimming motions, 18 points along the dorsal midline and two points from the lateral perspective for the tail depth were digitized using a computer (Commodore model Amiga 3000) and a dynamic-tracking U-matic video deck (Sony model BVU-9200). By electronically overlaying a paused video field (time resolution of 0.017 s) and an electronic cursor, we first manually selected seven landmarks on the axial midline (nose, anterior and posterior margins of pectoral fins, anterior margin of pelvic fins, site of first and second surgeries, and tip of caudal fin). We then evenly filled in the gaps between the landmarks with the remaining 11 points. Trials were digitized only when the individual achieved relatively constant velocity over three consecutive tailbeats (stable position in flow $\pm 0.02\,L$) and was positioned in the center of the tank. By failing to meet these criteria, the four (out of 84) missing cells described in the previous section were rejected.

Using the digitized midlines and tail depths for each individual, speed and skin treatment, we measured seven kinematic variables: tailbeat amplitude, tailbeat frequency, propulsive wave speed, anterior and posterior propulsive half-wavelengths, tail depth and maximal curvature at the site of the first (dermis cut; caudal curvature) and third (precaudal scale; precaudal curvature) surgical treatments. Tailbeat amplitude (in L), was half the peak-to-trough lateral displacement of the tip of the tail. Tailbeat frequency (in Hz) was the inverse of the period of the tailbeat cycle (in s). Propulsive wave speed (in $L\,s^{-1}$) was the product of the tailbeat frequency and twice the posterior half-wavelength. The anterior and posterior half-wavelengths (in L) were the half-wave components of the propulsive wave, a standard kinematic variable that is the apparent wavelength of the body when midline images, with the tail tip at its maximum lateral excursion, are superimposed about the axis of progression (Webb *et al.* 1992). Tail depth (in L) was the maximum distance between the dorsal- and ventralmost points of the trailing edge of the caudal fin when viewed laterally. Maximal curvature of the axial midline (in m^{-1}) at the surgical sites was determined using trigonometry. First, the radius of curvature, R (in m), of the midline at each surgical site on each video image was calculated using the following formula:

$$R = \frac{D}{4[\cos(\theta/2)]}\,, \tag{3}$$

where θ is the angle formed between two segments of total length, D, on the axial midline. The angle was determined from the law of cosines and the x,y-coordinates of the digitized point at the surgical site and a point on either side also falling on the midline. The total segment length, the distance on the midline between the three points, was calculated from the Pythagorean theorem. The midline curvature is the inverse of the radius of curvature.

In addition, the relative total hydrodynamic power, P, or relative rate of working of the propulsive wave, was calculated. According to Lighthill's elongated-body theory (Lighthill, 1975), relative total power is proportional to the following variables (Wu, 1977):

$$P \propto F^2H^2B^2\left(1 - \frac{u}{F\lambda}\right), \tag{4}$$

where F is the tailbeat frequency (in Hz), H is the tailbeat amplitude (in m), B is the depth of the trailing edge of the caudal fin in the sagittal plane (in m), u is the swimming speed (in $m\,s^{-1}$) and λ is the propulsive wavelength of the body (in m). Note that the product of tailbeat frequency, F, and propulsive wavelength, λ, is the speed of the propulsive wave, c. The speed of the propulsive wave was also calculated, since it is predicted to be proportional to the flexural stiffness of the body (McHenry *et al.* 1995; Long and Nipper, 1996) and, relative to the forward swimming speed, determines the propeller or Froude efficiency (see Cheng and Blickhan, 1994; Webb *et al.* 1984).

Results

Flexural stiffness

In the region of the caudal scale row (see Fig. 1), sequential alteration of the skin increases the neutral zone of curvature and decreases the flexural stiffness of the body (Fig. 4A). For three individuals, the neutral zone of curvature ranged from a mean of $10\,m^{-1}$ in unaltered gar to a mean of $13\,m^{-1}$ with the caudal scale row removed (Table 1; Fig. 4B). The flexural stiffness of the body decreased from a mean of $0.065\,N\,m^2$ in unaltered gar to a mean of $0.050\,N\,m^2$ in gar with the caudal scale row removed (Table 1; Fig. 4C). For both the neutral zone of curvature and flexural stiffness, the only significant differences occurred when the dermis was cut.

Kinematics of steady swimming

When the skin was altered, tailbeat amplitude, tailbeat frequency, wave speed and tail depth showed significant overall effects (Table 2). When live gar had their dermis cut posterior to the caudal scale row, tailbeat frequency decreased across the range of swimming speeds (Fig. 5A), tail depth

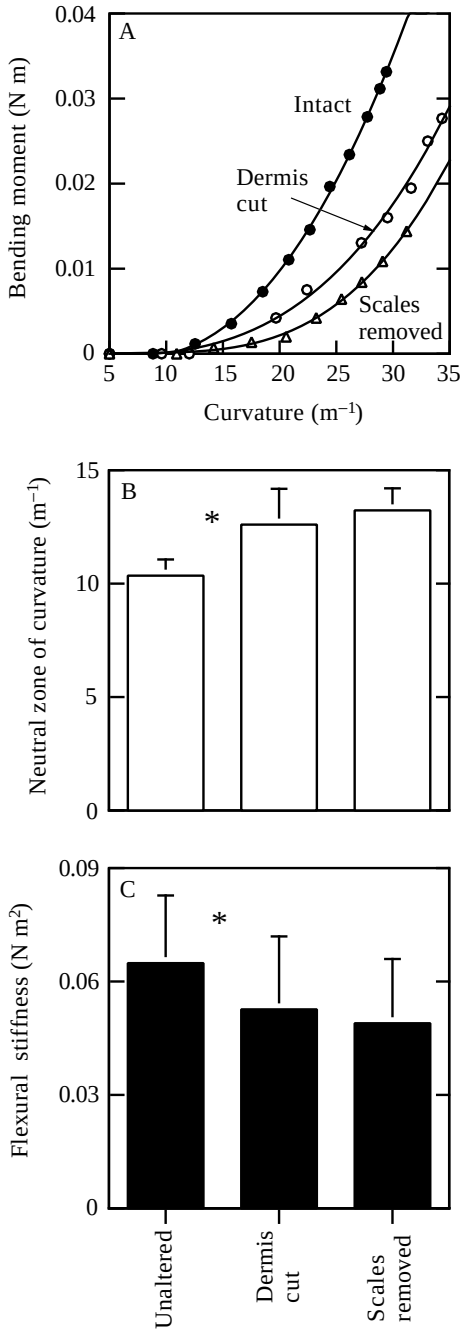

Fig. 4. Flexural stiffness of longnose gar *Lepisosteus osseus*, with pre- and post-operative conditions compared. (A) Typical loading curves, showing differences in the neutral zone of curvature (see Fig. 3) and the slope of the lines in a single gar with skin intact (filled circles), dermis cut (open circles) and scale row removed (filled triangles). (B,C) Mean values compared (means +1 S.E.M., N=3 individuals). (B) The neutral zone of curvature increases significantly when the dermis is cut. Note that the trend is for the neutral zone to increase as the scale row is removed (significant overall effect in ANOVA; see Table 1). (C) The mean of the flexural stiffness of the body 10 m^{-1} past the end of the neutral zone is significantly lower when the dermis is cut. Note that the trend is for the flexural stiffness to continue to decrease when the scale row is removed (significant overall effect in ANOVA; see Table 1). Pairwise comparisons of means made with planned *a priori* contrasts (* indicates a significant difference between two values, P<0.05).

Table 1. *Summary of* F*-values (Type III sums of squares) from ANOVAs performed separately on flexural stiffness variables of* Lepisosteus osseus *bodies*

Variable	Individual (2)	Skin (2)
Neutral zone	16.17 (0.0121)	10.63 (0.0251)
Flexural stiffness	152.31 (0.0002)	10.86 (0.0242)

P-values are indicated in parentheses to the right of each value of *F*.

Degrees of freedom (d.f.) are given to the right of each factor; error d.f. were 4.

The factor 'Individual' was treated as a randomized block effect without replication; therefore, no interaction term using that factor could be run.

increased (Fig. 5B) and wave speed decreased (Fig. 5C). In addition, tailbeat frequency increased linearly with increasing swimming speed (Table 2); this relationship can be described by linear regression of the mean tailbeat frequency against speed for gar with unaltered skin (N=7, r^2=0.804) as y=0.975+1.655x and for gar with dermis cut (N=7, r^2=0.932) as y=0.809+1.531x, where x is the swimming speed (L s^{-1}) and y is the tailbeat frequency (Hz). Tail depth did not vary significantly with changes in swimming speed (Table 2). Wave speed, the product of the tailbeat frequency and twice the posterior half-wavelength, also increased linearly with increasing swimming speed; this relationship can be described, by linear regression, for gar with unaltered skin (N=7; r^2=0.854) as y=0.457+0.972x and for gar with dermis cut (N=7, r^2=0.957) as y=0.229+0.871x, where x is the swimming speed (L s^{-1}) and y is the wave speed (L s^{-1}).

When live gar had the caudal scale row removed, the mean values of tailbeat amplitude, wave speed and relative total power (pooled across swimming speed) increased relative to the dermis cut values, by 25 %, 29 % and 64 %, respectively. Note that the increase in relative total power, independent of swimming speed, indicates that the percentage thrust (fraction of useful power) generated by the undulatory wave has decreased. When the precaudal scale row was removed, no significant changes were detected.

While showing no significant changes when the dermis was cut, four variables changed significantly with swimming speed (Table 2; Fig. 6). Tailbeat amplitude increased with increasing swimming speed (Fig. 6A) in a manner described by the following regression equation for gar with unaltered skin (N=7; r^2=0.612), y=0.091+0.018x, and for gar with dermis cut (N=7, r^2=0.321) y=0.072+0.034x, where x is the swimming speed (L s^{-1}) and y is the tailbeat amplitude (L). Relative total power increased with increasing swimming speed (Fig. 6B) in a manner described by the following regression equation for gar with unaltered skin (N=7;

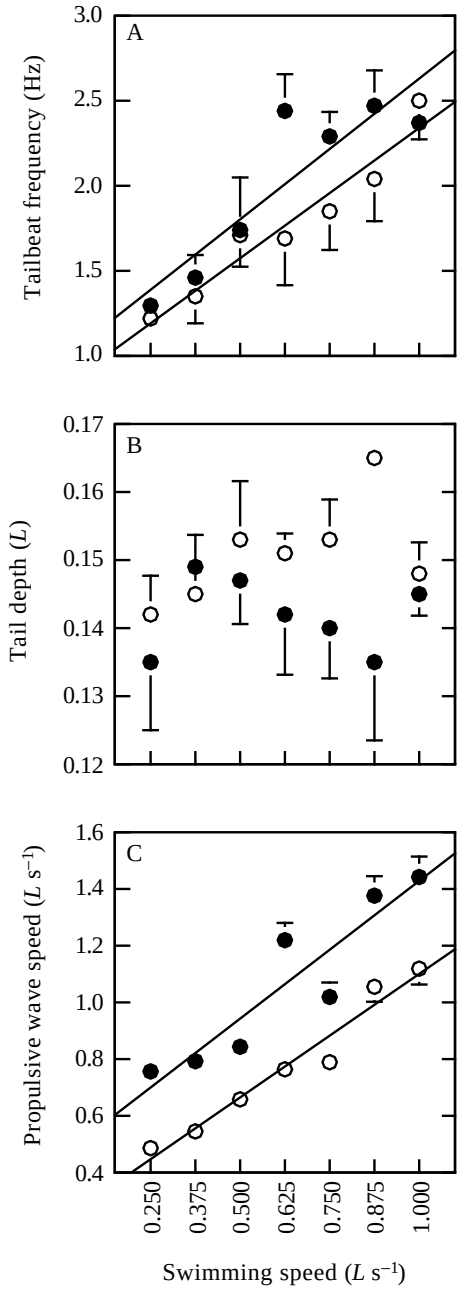

Fig. 5. Kinematic variables that differ significantly when the dermis is cut (see Table 2). Each point is the mean (±1 S.E.M.) from three individuals. Filled circles are from intact fish, while open circles are from those whose dermis has been cut. (A) Tailbeat frequency. When the dermis is cut, the tailbeat frequency decreases significantly over the entire range of speeds. Since the flexural stiffness of the body decreases when the dermis is cut (see Fig. 4C), this result supports the prediction that the body's flexural stiffness determines, in part, the cycle frequency at which the gar chooses to operate. (B) Tail depth. When the dermis is cut, tail depth increases significantly. Given that relative hydrodynamic power remains constant (see Table 2), the increased tail depth compensates for the reduced tailbeat frequency at any given speed (see equation 4). (C) Propulsive wave speed. When the dermis is cut, wave speed decreases significantly. Since wave speed is the product of tailbeat frequency and propulsive wavelength (see Fig. 7), and tailbeat frequency decreases significantly (see A), it is not surprising that wave speed decreases as well. *L*, body length.

r^2=0.812), y=–0.095+13.667x, and for gar with dermis cut (N=7, r^2=0.604) y=–3.070+18.483x, where x is the swimming speed ($L\,s^{-1}$) and y is the relative total power ($\times10^{-9}$). While there was a significant overall effect of speed on maximal curvature of the axial midline (Table 2; Fig. 6C,D), planned contrasts detected a significant effect only between speeds of 0.250 and 0.375 $L\,s^{-1}$.

The only kinematic variables for which no significant effect of skin treatment or swimming speed could be detected were the anterior and posterior half-wavelengths (Table 2; Fig. 7). The mean value of the anterior half-wavelength was 0.335±0.0426 L (±S.E.M.; N=28 with individuals pooled). The mean value of the posterior half-wavelength was 0.276±0.0291 L (±S.E.M.; N=28 with individuals pooled).

Finally, for all the kinematic variables except anterior half-wavelength and wavespeed there were significant individual effects (Table 2). Since we were interested in generalizing our results across individuals, these effects were not explored further. Note that individual effects do not influence the significant results for skin treatment and swimming speed; this is analogous to treating individual as a randomized block effect without replication (Sokal and Rohlf, 1981).

Discussion

In the mechanics of undulatory swimming, the skin of longnose gar plays an integral role: it passively stiffens the body, and the magnitude of this stiffness, in turn, influences the cycle frequency and propulsive wave speed at which the gar chooses to operate. Support for this hypothesis comes from experiments involving *in vivo* surgical manipulation of skin structure and *in situ* measurement of the flexural stiffness of the body.

Locomotor functions of gar skin

The present experiments are the first to test, in live fish, the hypothesis that flexural stiffness of the body alters swimming mechanics (Blight, 1976, 1977; Long *et al.* 1994; McHenry *et al.* 1995) in a manner consistent with engineering theory of forced, harmonically oscillating beams (see Den Hartog, 1956; Long and Nipper, 1996). As predicted, when the dermis is cut between two caudal scale rows (Figs 1, 2), the passive flexural stiffness decreases (Fig. 4C) and the tailbeat frequency and propulsive wave speed decrease (Fig. 5A,C). This hypothesis has also been supported in swimming experiments on dead, electrically stimulated sunfish (Long *et al.* 1994) and flexible sunfish models (McHenry *et al.* 1995). Thus, in the case of longnose gar, it appears that the skin, and the dermis in particular, functions to stiffen the body – passively – and hence increase the tailbeat frequency at which the gar chooses to operate. Tailbeat frequency, in turn, controls the propulsive wave speed, and both variables are

Table 2. *Summary of* F*-values (Type III sums of squares) from ANOVAs performed separately on kinematic variables of gar swimming with and without altered skin*

Variable	Individual (2)	Skin (3)	Speed (6)	Skin × speed (18)
Tailbeat amplitude	9.77 (0.0003)	3.16 (0.0325)	3.00 (0.0138)	0.76 (0.7345)
Tailbeat frequency	9.22 (0.0004)	4.14 (0.0106)	16.64 (0.0001)	0.81 (0.6776)
Anterior wavelength	0.41 (0.6688)	0.43 (0.7316)	0.53 (0.7827)	0.69 (0.8082)
Posterior wavelength	7.92 (0.0010)	0.90 (0.4494)	0.18 (0.9805)	0.59 (0.8911)
Propulsive wave speed	0.44 (0.6452)	3.28 (0.0282)	6.47 (0.0001)	0.29 (0.9970)
Tail depth	37.17 (0.0001)	4.35 (0.0085)	0.94 (0.4767)	0.65 (0.8446)
Precaudal curvature	29.11 (0.0001)	0.35 (0.7861)	2.66 (0.0254)	0.93 (0.5447)
Caudal curvature	23.76 (0.0001)	0.65 (0.5881)	3.47 (0.0060)	0.39 (0.9839)
Relative power*	66.90 (0.0001)	2.47 (0.0727)	16.54 (0.0001)	0.57 (0.9031)

P-values are indicated in parentheses to the right of each value of *F*.

Degrees of freedom (d.f.) are given to the right of each factor; error d.f. were 50.

The factor 'Individual' was treated as a randomized block effect without replication; therefore, no interaction term using that factor could be run.

*Relative power was log-transformed to normalize its distribution. The results from the transformed analyses are given here. The untransformed data yielded the same qualitative results.

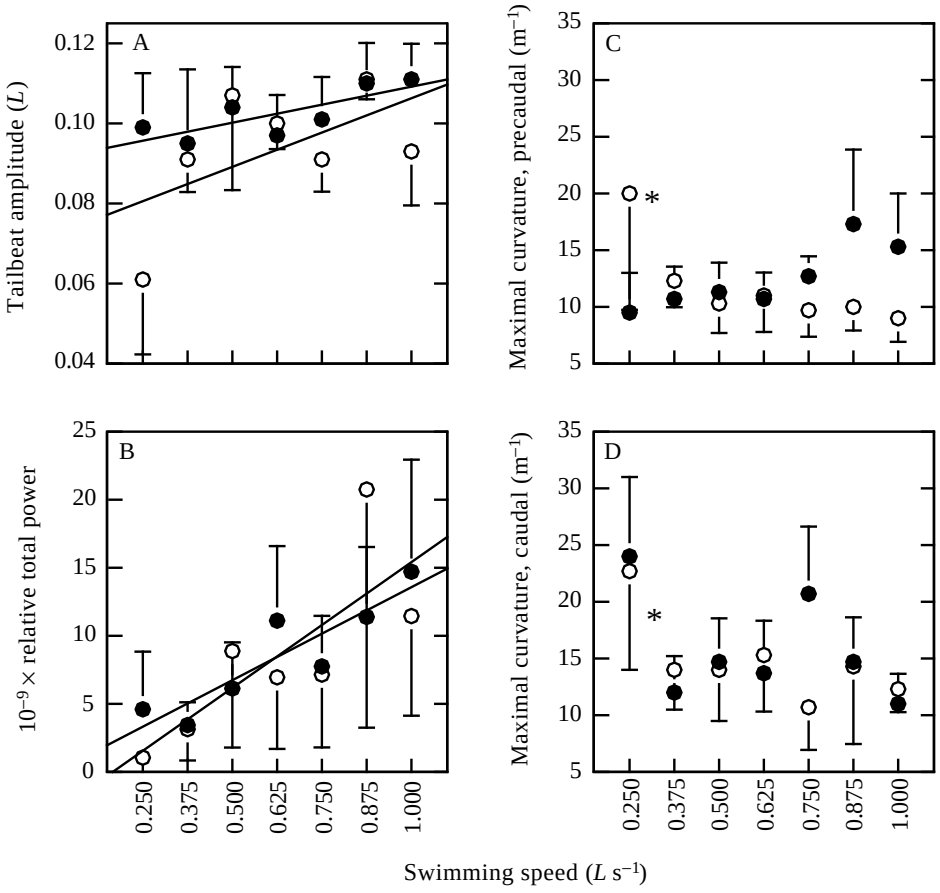

Fig. 6. Kinematic variables that differ significantly with changes in swimming speed (see Table 2). Each point is the mean (±1 S.E.M.) of three individuals. Filled circles are from intact fish, while open circles are from those whose dermis has been cut. For regression equations, see Results. Note that, even though the data are presented separately, no significant differences were detected between values for gar with skin intact or with dermis cut. (A) Tailbeat amplitude increases significantly with increasing swimming speed (Table 2). (B) Relative total power increases significantly with increasing swimming speed (Table 2). (C) Maximal midline curvature at dorsal position of precaudal scale row treatment decreases significantly between speeds of 0.250 and 0.375 $L\,s^{-1}$, where L is body length. (D) Maximal midline curvature at dorsal position of caudal scale row treatment decreases significantly between speeds of 0.250 and 0.375 $L\,s^{-1}$. An asterisk indicates a significant difference between values at two adjacent swimming speeds (P<0.05).

important in the production of thrust power by the undulatory wave (see equation 4).

The kinematic changes caused by cutting the dermis approach theoretical expectations for a passively stiff system. The proportional decreases in tailbeat frequency (mean 2.04–1.77 Hz, pooled across swimming speed, a 13 % reduction, see Fig. 5A) and propulsive wave speed (mean 1.08–0.77 $L\,s^{-1}$, pooled across swimming speed, a 29 % reduction, see Fig. 5C) are similar to the decrease in flexural stiffness (mean 0.065–0.053 $N\,m^2$, an 18 % reduction, see Fig. 4C). The theory of mechanical vibrations predicts a non-linear relationship between the resonance frequency of a

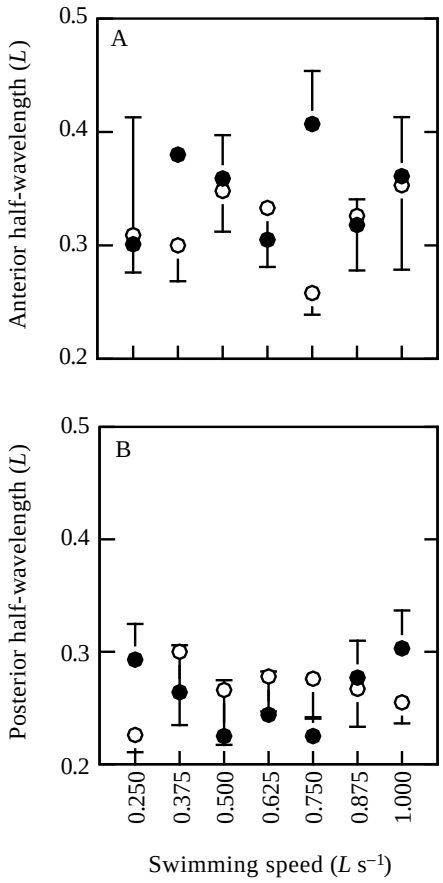

Fig. 7. Kinematic variables for which no significant effects of skin treatment or swimming speed could be detected (see Table 2). Each point is the mean (±1 S.E.M.) from three individuals. Filled circles are from intact fish, while open circles are from those whose dermis has been cut. Note that, even though the data are presented separately, no significant differences were detected between values for gar with skin intact or with dermis cut. (A) Anterior propulsive half-wavelength. (B) Posterior propulsive half-wavelength. *L*, body length.

structure and its stiffness (Den Hartog, 1956; Denny, 1988). If we equate resonance and tailbeat frequency, *F*, then we expect the following:

$$F \propto \sqrt{EI}. \quad (5)$$

The ratio of the tailbeat frequency to the square root of the flexural stiffness, *EI*, should remain constant if neither mass nor damping change; note that the use of this simple proportionality assumes that the gar is choosing to operate at or near its resonance frequency, where the mechanical cost of bending would be minimized (for further discussion, see Long and Nipper, 1996). If we compare the ratio of tailbeat frequency to the square root of flexural stiffness for the two treatments, averaging across swimming speeds, we find only a 4% difference (8.00 for the intact treatment and 7.69 for the dermis cut treatment). At the same time, the ratio of wave speed to the square root of flexural stiffness yields a difference of 26% (4.24 for the intact and 3.34 for dermis cut treatment). In both cases, these ratios decrease with the cutting of the dermis, suggesting that the effective flexural stiffnesses are higher than expected in a passive-stiffness system. This extra flexural stiffness may be provided actively by negative muscle work (see McHenry *et al.*1995), which may be produced during part of the tailbeat cycle in fish (for a review, see Wardle *et al.* 1995, but see also Jayne and Lauder, 1995*a*; Rome *et al.* 1993). To test this hypothesis in gar, muscle activity patterns could be measured electromyographically in intact gar and in gar with the dermis cut; a difference in activity phase relative to local body bending would support the hypothesis that muscle activity is modulated to enhance flexural stiffness.

If, at any single swimming speed, tailbeat frequency decreases when the dermis is cut, how are surgically altered gar able to generate enough hydrodynamic power to maintain their speed? Gar compensate for the loss of hydromechanical power (see equation 4) by increasing tail depth (Fig. 5B), which maintains the relative total power at any given swimming speed (Fig. 6B).

In addition to the importance of the dermis, the functions of the skin of gar may also depend on the scale rows. In polypterid fish, which also possess bony ganoid scales, Pearson (1981) has suggested that the dermis resists axial tension, that the scale rows resist axial compression and that the dermis and scale rows function together to resist axial torsion. It is reasonable to assume that the same principles operate in longnose gar, since their dermis and scale rows are similar in construction and arrangement to those of polypterids (Kerr, 1952). In gar, when the caudal scale row is removed, the tailbeat amplitude, wave speed and relative hydrodynamic power increase. Since removal of the scale row does not, however, alter the bending properties of the body (Fig. 4), it is difficult to interpret the functional significance of the associated kinematic changes. In addition to the resistance of axial compression (Pearson, 1981), scale rows may also function to resist medio-lateral compression applied by the underlying muscles. In mackerel and tuna, which lack ganoid scales, internal muscle pressure may resist medio-lateral compression of the body, allowing the muscles to use the skin and its associated connective tissues as a pulley for the myotomes (Westneat *et al.* 1993). In seahorses, the unusual axial muscles attach directly to the dermal plates which, in turn, are connected to the backbone; muscle contraction in the tail thus appears to bend the body by transmitting forces directly to the dermal structures (Hale, 1996). The myomeres of gar are attached to the scales by discrete connections (Fig. 2); a single hypaxial myotome attaches to several scale rows epaxially and a single scale row hypaxially (Gemballa, 1995). Muscle pressure may not be needed to resist compression in species with ganoid scales, since the robust and bony scales are tightly bound within a scale row and provide substantial resistance to circumferential deformation (Kerr, 1952; Pearson, 1981; Brainerd, 1994; Gemballa, 1995). Thus, on the basis of this structural organization, we propose that a gar's scale row resists medio-lateral forces, providing myomeres with leverage and anchorage for pulling serial tendons and

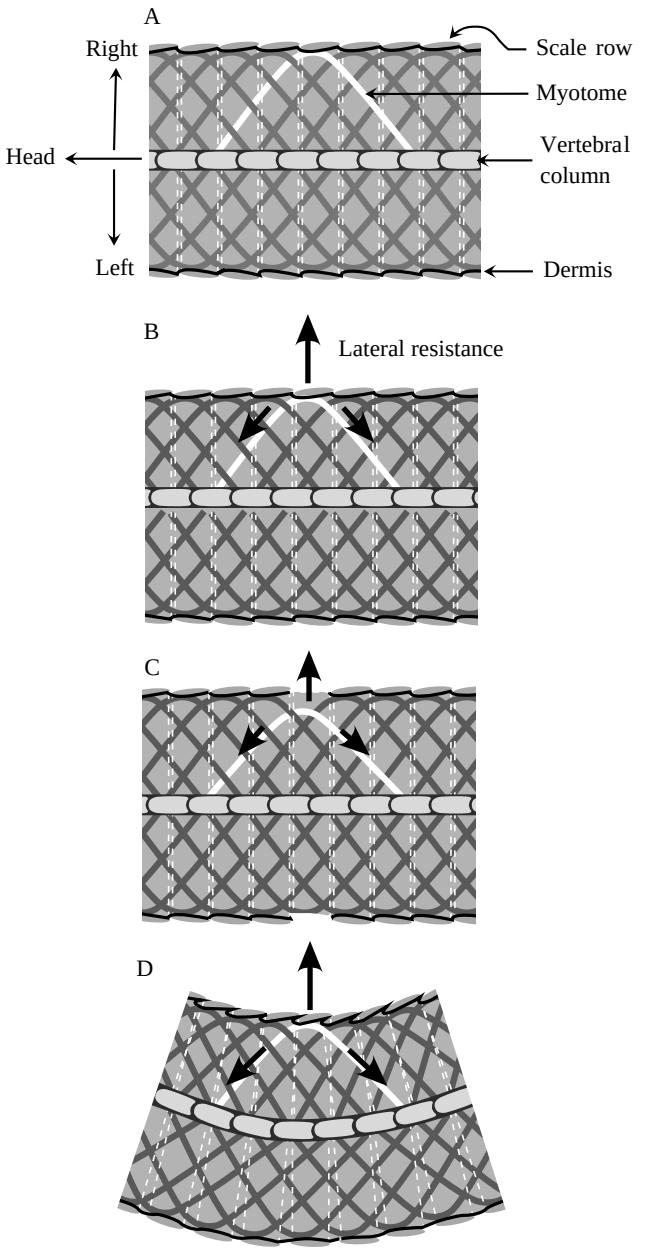

Fig. 8. Hypothetical scale function model for gar skin. Frontal (horizontal) view of body at the level of the horizontal septum. (A) Illustration of the musculo-skeletal anatomy of the body axis. The scale rows are the lateralmost structures and are attached to the dermis, which spans the gap between scale rows and attaches to the underlying musculature at the myotome pathway. The myotome pathway represents the muscle/tendon trajectory described in Westneat *et al.* (1993) for scombrids. The anterior half of the pathway is presumed to be pulled upon by the myomere to which it is attached. The dashed white vertical lines represent the continuation of the scale rows out of the plane of the figure and following the circumference of the body. (B) When a given myomere contracts, the scale row resists compression (large vertical arrow), which allows the myomere to exert a bending moment on the body anteriorly and posteriorly (large diagonal arrows). (C) Without resistance from a scale row, the myomere cannot exert as large a bending moment with the same input of force, since its moment arm (distance from lateralmost attachment site to vertebral column) has been reduced. (D) With the scale row intact, the moment arm of the muscle is larger and the body can be bent more forcefully.

bending the body (Fig. 8). If this is how the scale row functions, its removal might possibly have caused the changes in swimming kinematics detected in this study. However, our experimental design does not test this model. To do so properly, muscle–skin attachments or medio-lateral stiffness would need to be altered while the relationship between muscular bending moments and body bending during swimming was directly measured.

The final experimental treatment yielded intriguing results. When the precaudal scale row was removed, the swimming kinematics did not change. Even though the effect of this treatment on flexural stiffness was not measured, it is reasonable to predict that the associated simultaneous loss of dermal connection and muscle attachment should lower bending stiffness in a manner similar to that described for the caudal skin treatments (Fig. 4). However, the precaudal region of gar does not bend as much as the caudal region beyond the neutral zone of curvature (compare Fig. 4B with Fig. 6C). Thus, the precaudal region of the body never bends enough to be influenced by the lower flexural stiffness caused by the cutting of the dermis and removal of the scale row; hence, the function of the skin may vary regionally.

Mechanics of fish skin

As far as we know, these are the first measurements of the flexural stiffness of fish skin *in situ*. From the measurement of a substantial neutral zone (Fig. 4B), it appears that the skin of unaltered longnose gar permits bending at small curvatures and resists bending at high curvatures. Maximal curvature of the axial midline (Fig. 6D, caudal scale row), is approximately $15\,m^{-1}$ at most swimming speeds; this is approximately $5\,m^{-1}$ beyond the neutral zone of curvature of $10\,m^{-1}$ (Fig. 4B). Thus, the flexural stiffness of the skin beyond the neutral zone (Fig. 4C) functions to decelerate the lateral motion of the body. In this way, the skin passively performs a function, deceleration, that might otherwise be muscularly controlled; it does so without incurring additional mechanical work over much of the tail stroke because of the neutral zone.

How is skin organized to create both a neutral zone and bending resistance? The dermis connecting adjacent scale rows appears to play a key role (Fig. 2), since its absence significantly increases the neutral zone and decreases flexural stiffness (Fig. 4B,C). At low curvatures, it appears that the dermis is slack on both the concave and convex sides of the body. The low resistance of the neutral zone ends when the dermis is placed in tension, and resistance to bending is developed. In this model, which is similar to that developed by Pearson (1981) for polypterid fishes, the function of the bony ganoid scales is to resist compressive forces (Fig. 8). As our bending data show, however, the scale rows are necessary but not sufficient for significantly greater flexural stiffness

(Fig. 4C). Our model of axial skin strain in gar is different from, but complementary to, that for circumferential strain developed by Brainerd (1994) for polypterids. In polypterids, the tissues *within* scale rows store elastic energy, with the connective tissues deforming and recoiling as cross-sectional shape changes during lung ventilation (Brainerd, 1994). In gar, the tissues *between* scales rows determine the important mechanical properties. It is likely that both models apply only to fishes with armored or heavily scaled skin.

The gar's axial musculo-skeletal system is unusual in its lateral flexibility. When the dermis is cut and the caudal scale row is removed, the remaining muscle and backbone still show a neutral zone (Fig. 4). This is a surprising result, given that the backbones of other fishes show no such neutral zone (Hebrank, 1982; Hebrank *et al.* 1990; Long, 1992; J. H. Long, 1995). Gars are the only fish with opisthocoelous joints, with the centrum convex anteriorly and concave posteriorly (Goodrich, 1930). In a manner yet to be determined, this unusual intervertebral joint design may play a role in creating the neutral zone. Neutral zones are also present in the intervertebral joints of mammals, which possess an intervertebral joint with flat articular surfaces on the centra; Gal (1993) describes a range of neutral zones from 2 to 18 ° in rabbits and seals, respectively, with intermediate values for monkey, wallaby, tiger and jaguar.

Control of swimming speed

An excellent predictor of swimming speed in gar is the speed of the propulsive wave (Fig. 5C). If, as we propose above, wave speed is determined by the passive and active stiffness of the body, then we would predict that the range of steady swimming speeds is modulated by muscles generating negative work and, in consequence, stiffening the body. The alternative hypothesis is that flexural stiffness remains constant and that the muscles increase mechanical power output solely through increased positive work. Tests of these hypotheses await our ability to measure *in vivo* muscle force.

Evolutionary scenarios for the reduction of armored skin

The first vertebrates, which appeared some 450 million years ago, are characterized by the presence of external, dermal bone (J. A. Long, 1995). An extensive exoskeleton is clearly seen in the oldest complete fossil fish, *Sacabambaspis*, with articulated plates, oriented in obliquely inclined scale rows, covering the body (J. A. Long, 1995). While the first robust exoskeletons are often interpreted as adaptations against predation (e.g. J. A. Long, 1995; Carroll, 1988), the presence of ganoid scales in living gar and polypterids has other mechanical consequences, including enhanced station-holding (Webb *et al.* 1992) and passive lung inflation (Brainerd *et al.* 1989; Brainerd, 1994). Furthermore, the results of this study demonstrate that armored skin can play a central role in the control of body stiffness and undulatory wave motion during steady swimming. Hence, any 'how-possibly' explanation (*sensu* Brandon, 1990) of early vertebrate adaptations should consider that armored skin may represent an *alternative* rather than a maladaptive solution to the evolutionary challenges of aquatic locomotion.

The authors wish to thank Julia Parrish, Steve Vogel and Carlton Heine for the design and fabrication of the flow tank, Charles Pell for the design of the bending grips, Bill Kirby-Smith for logistical support at the Duke Marine Laboratory, and Bart Shepherd, Robert Suter, Steve Wainwright and two anonymous reviewers for constructive comments on the manuscript. J.H.L. and M.J.M. were supported by a grant to J.H.L. from the Office of Naval Research (N00014-93-1-0594). M.E.H. was supported by a Howard Hughes Predoctoral Fellowship. M.W.W. was supported by a grant from the National Science Foundation (IBN-9407253). Members of the Biomechanics Advanced Research Kitchen at Vassar College were instrumental throughout this project.

References

BLIGHT, A. R. (1976). Undulatory swimming with and without waves of contraction. *Nature* **264**, 352–354.

BLIGHT, A. R. (1977). The muscular control of vertebrate swimming movements. *Biol. Rev.* **52**, 181–218.

BRAINERD, E. L. (1994). Mechanical design of polypterid fish integument for energy storage during recoil aspiration. *J. Zool., Lond.* **232**, 7–19.

BRAINERD, E. L., LIEM, K. F. AND SAMPER, C. T. (1989). Air ventilation by recoil aspiration in polypterid fishes. *Science* **246**, 1593–1595.

BRANDON, R. N. (1990). *Adaptation and Environment*. Princeton, NJ: Princeton University Press.

CARROLL, R. L. (1988). *Vertebrate Paleontology and Evolution*. New York: W. H. Freeman.

CHENG, J.-Y. AND BLICKHAN, R. (1994). Note on the calculation of propeller efficiency using elongated body theory. *J. exp. Biol.* **192**, 169–177.

DEN HARTOG, J. P. (1956). *Mechanical Vibrations*. 4th edn. New York: McGraw-Hill.

DENNY, M. W. (1988). *Biology and the Mechanics of the Wave-Swept Environment.* Princeton, NJ: Princeton University Press.

FUJII, R. (1968). Fine structure of the collagenous lamella underlying the epidermis of the goby *Chasmichthys gulosus. Annotnes zool. jap.* **41**, 95–106.

GAL, J. M. (1993). Mammalian spinal biomechanics. I. Static and dynamic mechanical properties of intact intervertebral joints. *J. exp. Biol.* **174**, 247–280.

GEMBALLA, S. (1995). Vergleichend-anatomische Untersuchungen am Lokomotionsapparat der Actinopterygii Phylogenetische Rekonstruktion und funktionelle Hypothesen. PhD dissertation, Universität Tubingen.

GOODRICH, E. S. (1930). *Studies on the Structure and Development of Vertebrates*. London: Macmillan.

HALE, M. E. (1996). Functional morphology of ventral tail bending and prehensile abilities of the seahorse. *J. Morph.* (in press).

HEBRANK, J. R., HEBRANK, M. R., LONG, J. H., JR, BLOCK, B. A. AND WAINWRIGHT, S. A. (1990). Backbone mechanics of the blue marlin *Makaira nigricans* (Pisces, Istiophoridae). *J. exp. Biol.* **148**, 449–459.

HEBRANK, M. R. (1980). Mechanical properties and locomotor functions of eel skin. *Biol. Bull. mar. biol. Lab., Woods Hole* **158**, 58–68.

HEBRANK, M. R. (1982). Mechanical properties of fish backbones in lateral bending and in tension. *J. Biomech.* **15**, 85–89.

HEBRANK, M. R. AND HEBRANK, J. H. (1986). The mechanics of fish skin: lack of an "external tendon" role in two teleosts. *Biol. Bull. mar. biol. Lab., Woods Hole* **171**, 236–347.

JAYNE, B. C. AND LAUDER, G. V. (1995*a*). Are muscle fibers within fish myotomes activated synchronously? Patterns of recruitment within deep myomeric musculature during swimming in largemouth bass. *J. exp. Biol.* **198**, 805–815.

JAYNE, B. C. AND LAUDER, G. V. (1995*b*). Red muscle motor patterns during steady swimming in largemouth bass: effects of speed and correlations with axial kinematics. *J. exp. Biol.* **198**, 1575–1587.

KERR, T. (1952). The scales of primitive living actinopterygians. *Proc. zool. Soc., Lond.* **122**, 55–78.

LIGHTHILL, M. J. (1975). *Mathematical Biofluiddynamics.* Res. Conf. Nat. Sci. Found., 1973, New York Soc. Ind. Appl. Math. SIAM.

LONG, J. A. (1995). *The Rise of Fishes*. Baltimore, Maryland: Johns Hopkins.

LONG, J. H., JR (1992). Stiffness and damping forces in the intervertebral joints of blue marlin (*Makaira nigricans*). *J. exp. Biol.* **162**, 131–155.

LONG, J. H., JR (1995). Morphology, mechanics and locomotion: the relation between the notochord and swimming motions in sturgeon. *Env. Biol. Fishes* **44**, 199–211.

LONG, J. H., JR, MCHENRY, M. J. AND BOETTICHER, N. (1994). Undulatory swimming: how traveling waves are produced and modulated in sunfish (*Lepomis gibbosus*). *J. exp. Biol.* **192**, 129–145.

LONG, J. H., JR, AND NIPPER, K. S. (1996). The importance of body stiffness in undulatory propulsion. *Am. Zool.* (in press).

MCHENRY, M. J., PELL, C. A. AND LONG, J. H., JR (1995). Mechanical control of swimming speed: stiffness and axial wave form in undulating fish models. *J. exp. Biol.* **198**, 2293–2305.

MOTTA, P. J. (1977). Anatomy and functional morphology of dermal collagen fibers in sharks. *Copeia* **1977**, 454–464.

NELSON, J. S. (1984). *Fishes of the World*. 2nd edn. New York: John Wiley & Sons.

PEARSON, D. M. (1981). Functional aspects of the skin in polypterid fishes. *Zool. J. Linn. Soc.* **72**, 93–106.

ROME, L. C., SWANK, D. AND CORDA, D. (1993). How fish power swimming. *Science* **261**, 340–343.

SAS INSTITUTE (1985). *SAS User's Guide: Statistics (version 5)*. Cary, North Carolina: SAS Institute, Inc.

SOKAL, R. R. AND ROHLF, F. J. (1981). *Biometry*. 2nd edn. New York: W. H. Freeman.

SUMMERFELT, R. C. AND SMITH, L. S. (1990). Anesthesia, surgery and related techniques. In *Methods for Fish Biology* (ed. C. B. Schreck and P. B. Moyle), pp. 213–272. Bethesda, MD: American Fisheries Society.

VIDELER, J. J. (1974). On the interrelationships between morphology and movement in the tail of the cichlid fish *Tilapia nilotica* (L.). *Neth. J. Zool.* **25**, 143–194.

VIDELER, J. J. (1993). *Fish Swimming*. London: Chapman & Hall.

VOGEL, S. (1981). *Life in Moving Fluids.* Boston: Willard Grant Press.

WAINWRIGHT, S. A., BIGGS, W. D., CURREY, J. D. AND GOSLINE, J. M. (1976). *Mechanical Design in Organisms*. New York: John Wiley & Sons.

WAINWRIGHT, S. A., VOSBURGH, F. AND HEBRANK, J. H. (1978). Shark skin: function in locomotion. *Science* **202**, 747–749.

WARDLE, C. S., VIDELER, J. J. AND ALTRINGHAM, J. D. (1995). Tuning in to fish swimming waves: body form, swimming mode and muscle function. *J. exp. Biol.* **198**, 1629–1636.

WEBB, P. W. (1993). The effect of solid and porous channels walls on steady swimming of steelhead trout *Onchorhynchus mykiss*. *J. exp. Biol.* **178**, 97–108.

WEBB, P. W., HARDY, D. H. AND MEHL, V. L. (1992). The effect of armored skin on the swimming of longnose gar, *Lepisosteus osseus*. *Can. J. Zool.* **70**, 1173–1179.

WEBB, P. W., KOSTECKI, P. T. AND STEVENS, E. D. (1984). The effect of size and swimming speed on locomotor kinematics of rainbow trout. *J. exp. Biol.* **109**, 77–95.

WESTNEAT, M. W., HOESE, W., PELL, C. A. AND WAINWRIGHT, S. A. (1993). The horizontal septum: mechanisms of force transfer in locomotion of scombrid fishes (Scombridae, Perciformes). *J. Morph.* **217**, 183–204.

WU, T. Y. (1977). Introduction to the scaling of aquatic animal locomotion. In *Scale Effects in Animal Locomotion* (ed. T. J. Pedley), pp. 203–232. New York: Academic Press.